Supporting Information

A facile template-assisted electrodeposition approach to porous Cu/Cu_2O nanowires

Jin Zhang[1,2‡], Jia Hao Ma[2,‡], Jingyuan Bai[3,*], Dalong Yang[1], Meilin Zhang[3], Zhou Yang[1], Longyi Fan[1], Xiao Lin Chen[1,2], Ren Guo Guan[1,*]

[1]*Engineering Research Center of Continuous Extrusion, Ministry of Education, Dalian Jiaotong University, Dalian 116028, P. R.China*

[2]*State Key laboratory of Solidification Processing, Center of Advanced Lubrication and Seal Materials, Northwestern Polytechnical University, Xi'an, Shaanxi, 710072, P. R. China*

[3]*School of Materials Science and Engineering, Northeastern University, Shenyang 110819, China;*

‡ both authors contributed equally to the work.

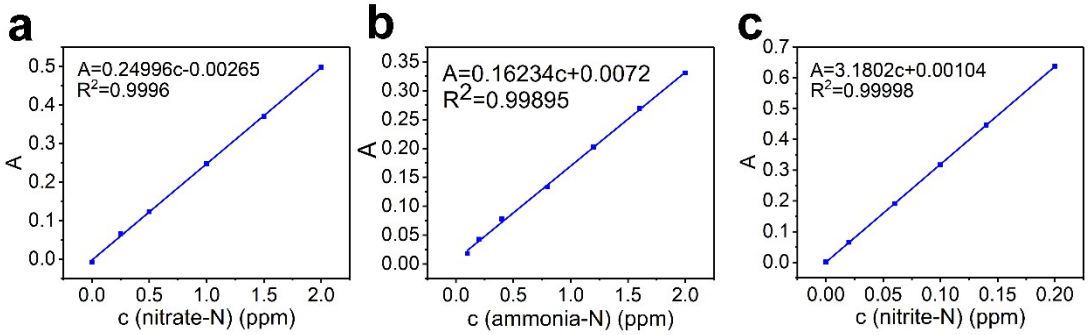

Figure S1. The UV-Vis absorption spectra and the corresponding calibration curves of a) nitrate-N, b) ammonia-N, c) nitrite-N for NO_3^- electroreduction measurements by using ultrapure water as background solution.

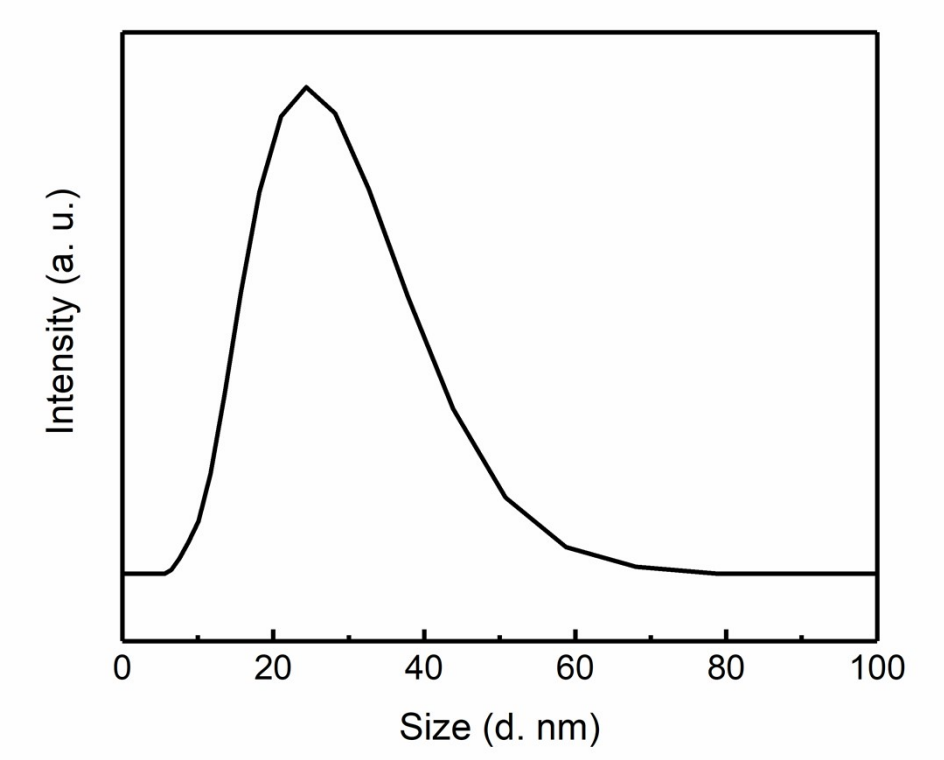

Figure S2. The size distribution of micelles in electrolyte containing 37g/L P-123 measured by dynamic light scattering (DLS).

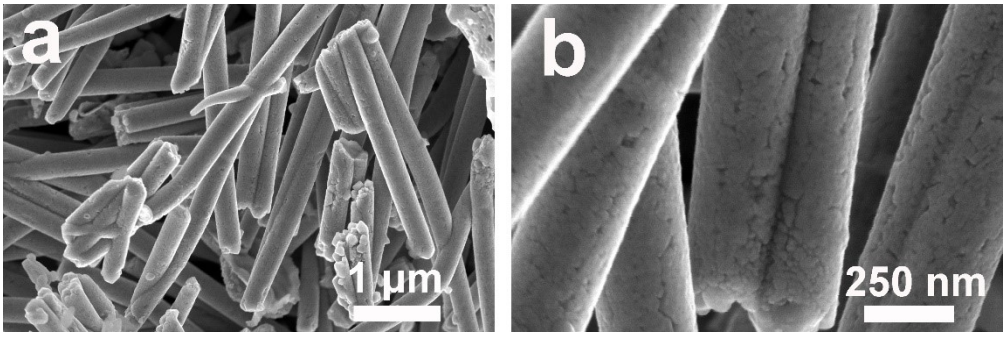

Figure S3. a) SEM and b) zoomed SEM images of as-obtained nanowires. The concentration of P-123 used is 8g/L.

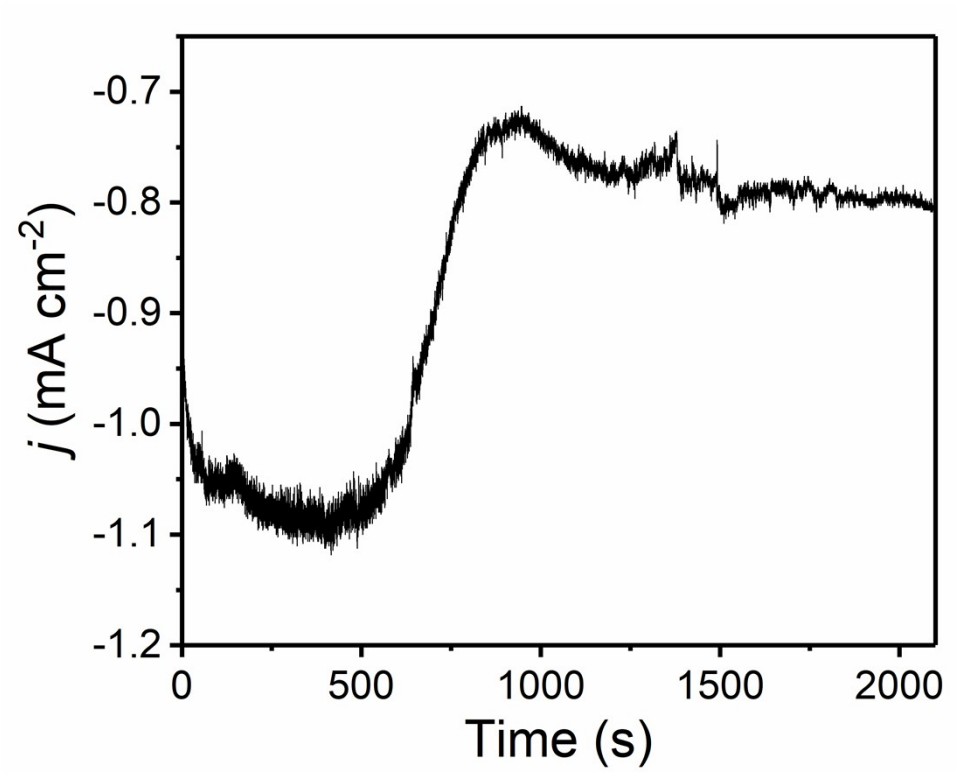

Figure S4. Current density changes during Cu/Cu_2O PNs eletrodeposition process.

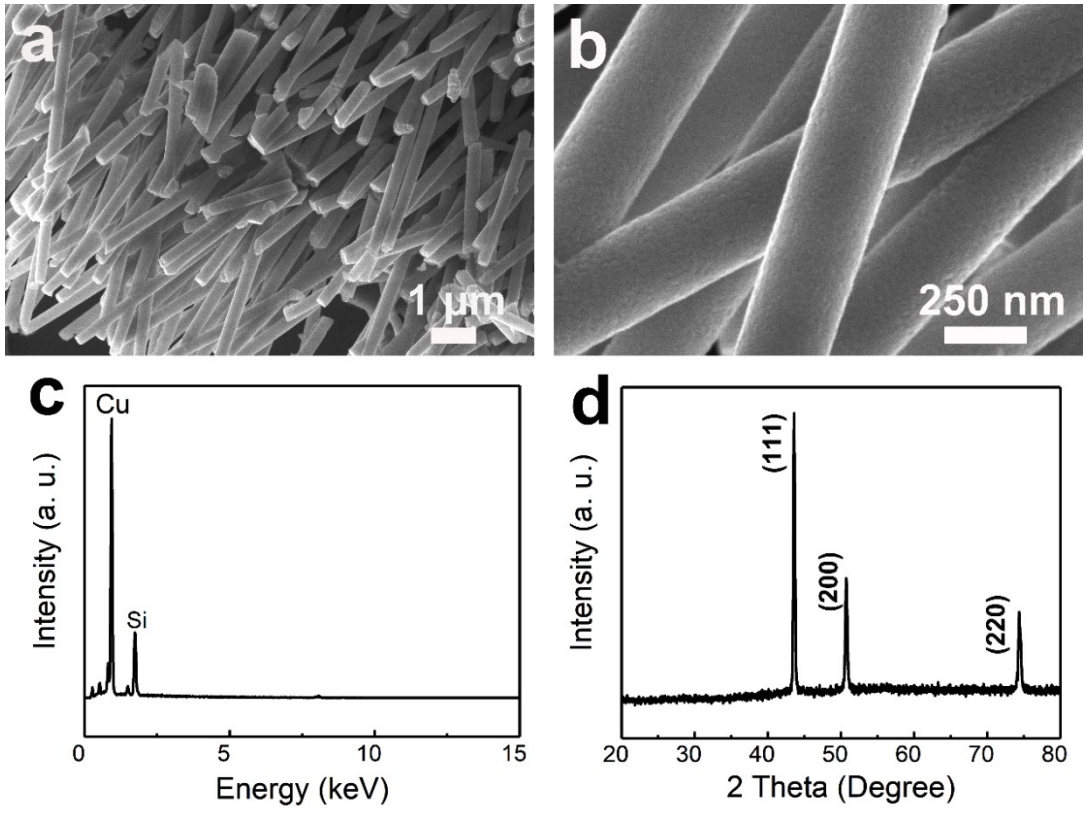

Figure S5. a) SEM, b) zoomed SEM, c) EDX d) XRD images of the Cu nanowires.

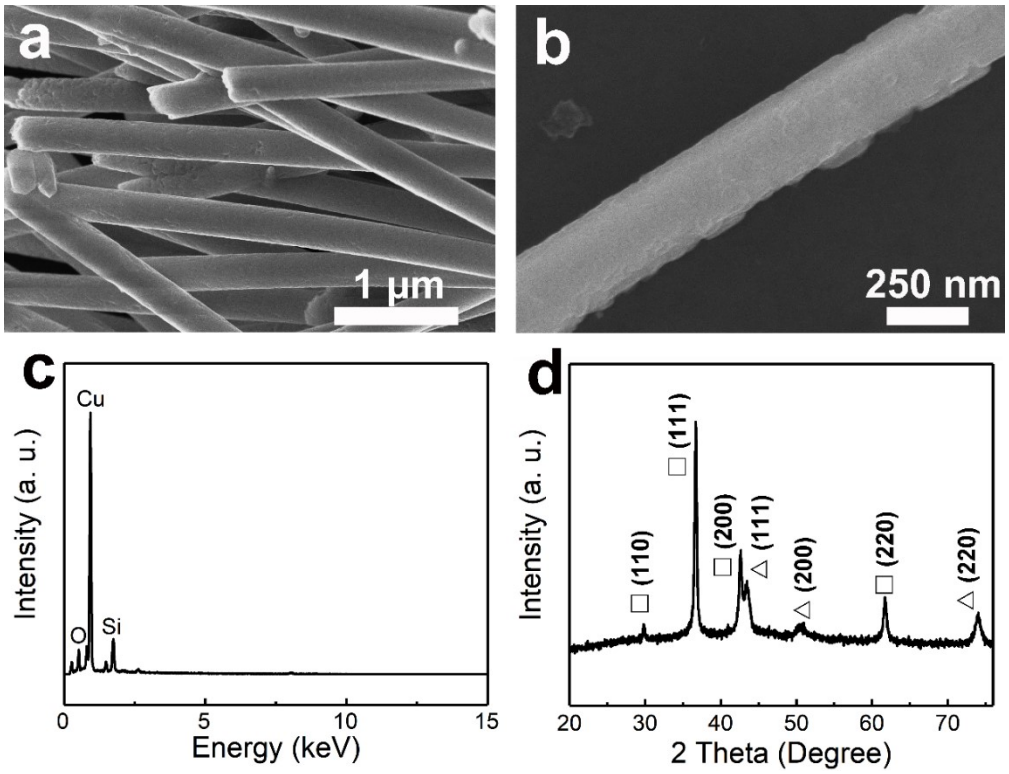

Figure S6. a) SEM, b) zoomed SEM, c) EDX d) XRD images of the Cu/Cu_2O nanowires. Peaks denoted Δ by □ belong to Cu and Cu_2O phases, respectively.

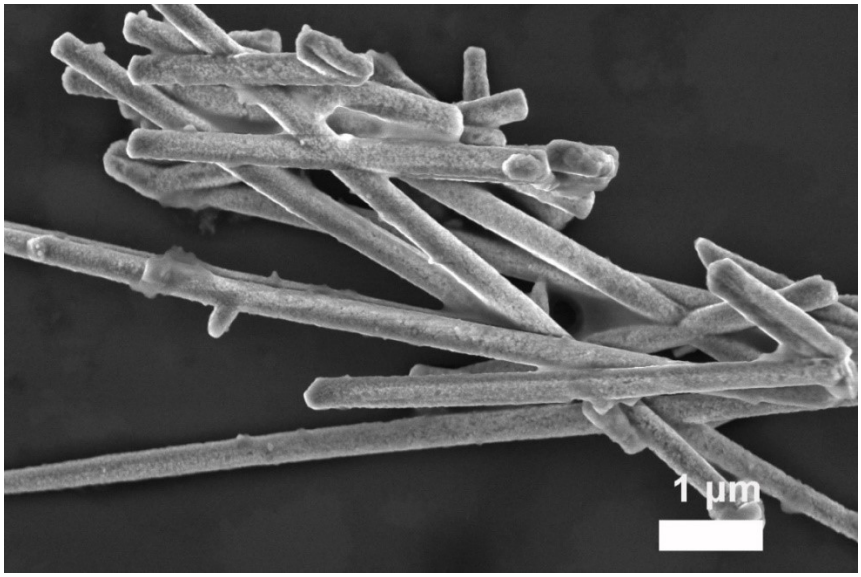

Figure S7. SEM image of the Cu/Cu_2O PNs after the electroreduction test.

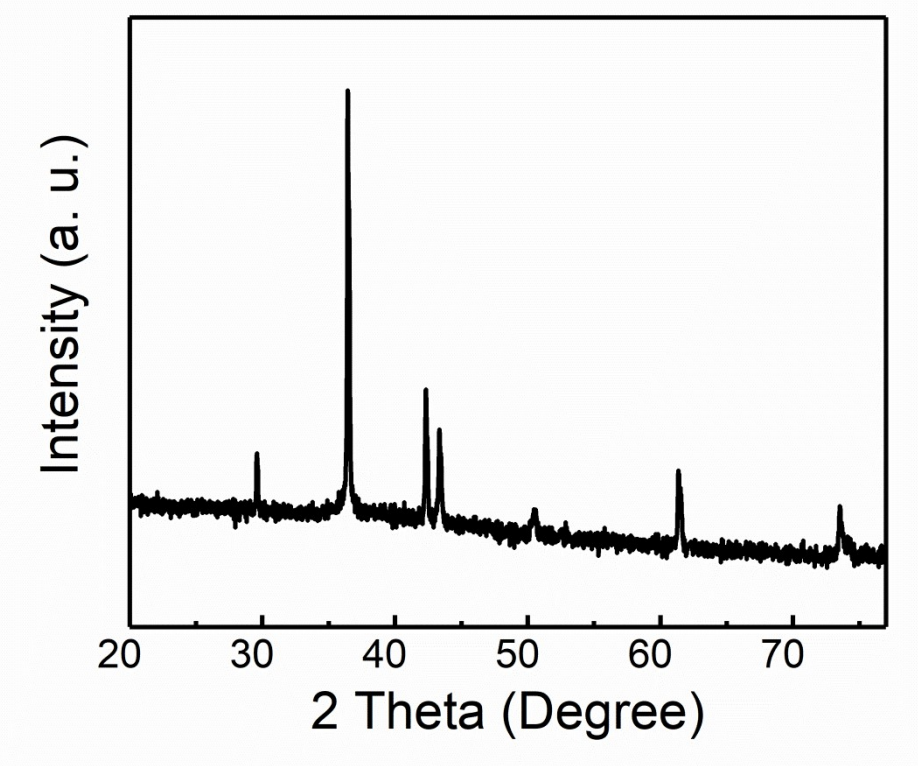

Figure S8. X-ray diffraction pattern of Cu/Cu_2O PNs after the electroreduction test.

Table S1. Comparison of NH_3 yield and ammonia selectivity by eletrocatalytic nitrate redction

Electrocatalyst	**Electrolyte**	**NH_3 yield**	**Ammonia selectivity**	**Ref**
Cu/Cu_2O porous nanowires	50 ppm NO_3^-+ 0.1 M K_2SO_4	2.73 mmol h^{-1} g^{-1}	37%	This work
CuO nanowire arrays	200 ppm NO_3^--N + 0.5 M Na_2SO_4	0.2449 mmol h^{-1} cm^{-2}	81.2%	1
Co_2O_3 nanorod arrays	100 g L^{-1} 0.1 M NO_3^-+ K_2SO_4	0.854 mmol h^{-1} cm^{-2}	33.6%	2
Fe single atom catalyst	0.5 M NO_3^-+ 0.1 M K_2SO_4	0.46 mmol h^{-1} cm^{-2}	75%	3
Cu–molecular solid catalyst	50 ppm NO_3^- +0.1 M PBS	436 ± 85 μg h^{-1} cm^{-2}	N.A. FE=85.9%	4
Co_3O_4@NiO	200 ppm NO_3^--N + 0.5 M Na_2SO_4	6.93 mmol $h^{-1}g^{-1}$	62.29%	5
Ir nanotube	0.1 M NO_3^-	921 μg h^{-1} mg_{cat}^{-1}	N.A. FE=84.7%	6
Ni_2P	80mg $L^{-1}NO_3^-$	0.056 mmol h^{-1}	89.1%	7

	-N + 0.5 M Na_2SO_4	mg^{-1}		
Ru/oxygen-doped-Ru core/shell nanoclusters t	mixed KOH/KNO_3 solution	5.56 mol g_{cat}^{-1} h^{-1}	~100%	8
Cu nanosheet	10 mM NO_3^- +0.1 M KOH	390.1μg mg^{-1}_{Cu} h^{-1}	N. A. FE=99.7%	9

1 Y. Wang, W. Zhou, R. Jia, Y. Yu, B. Zhang, *Angew. Chem. Int. Ed.* 2020, **59**, 5350.
2 Y. Wang, Y. Yu, R. Jia, C. Zhang and B. Zhang, *Natl. Sci. Rev*. 2019, **6**, 730.
3 Z. Y. Wu, M. Karamad, X. Yong, Q. Huang, D. A. Cullen, P. Zhu, C. Xia, Q. Xiao, M. Shakouri, F. Y. Chen, J. Y. Kim, Y. Xia, K. Heck, Y. Hu, M. S. Wong, Q. Li, I. Gates, S. Siahrostami, H. Wang, *Nat. Common*. 2021, **12**, 2870.
4 G. F. Chen, Y. Yuan, H. Jiang, S. Y. Ren, L. X. Ding, L. Ma, T. Wu, J. Lu, H. Wang, *Nat. Energy*, 2020, **5**, 605.
5 Y. Wang, C. Liu, B. Zhang, Y. Yu, *Sci. China Mater.* 2020, **63**, 2530.
6 J. Y. Zhu, Q. Xue, Y. Y. Xue, Y. Ding, F. M. Li, P. Jin, P. Chen, Y. Chen, *ACS Appl. Mater. Interfaces* 2020, **12**, 14064.
7 Q. Yao, J. Chen, S. Xiao, Y. Zhang, X. Zhou, *ACS Appl. Mater. Interfaces* 2021, **13**, 30458.
8 J. Li, G. Zhan, J. Yang, F. Quan, C. Mao, Y. Liu, B. Wang, F. Lei, L. Li, A. W. M. Chan, L. Xu, Y. Shi, Y. Du, W. Hao, P. K. Wong, J. Wang, S. X. Dou, L. Zhang, J. C. Yu, *J. Am. Chem. Soc*. 2020, **142**, 7036.
9 X. Fu, X. Zhao, X. Hu, K. He, Y. Yu, T. Li, Q. Tu, X. Qian, Q. Yue, M.R. Wasielewski, Y. Kang, *Appl. Mater. Today*, 2020, **19**, 100620